

Interband absorption in charged Ge/Si type-II quantum dots

A. I. Yakimov, N. P. Stepina, A. V. Dvurechenskii, and A. I. Nikiforov

Institute of Semiconductor Physics, Siberian Branch of the Russian Academy of Sciences, 630090 Novosibirsk, Russia

A. V. Nenashev

Novosibirsk State University, 630090 Novosibirsk, Russia

(Received 29 February 2000; revised manuscript received 22 May 2000; published 8 January 2001)

Using electron-filling modulation absorption spectroscopy, we study the effect of quantum dot charging on the interband excitonic transitions in type-II Ge/Si heterostructures containing pyramidal Ge nanocrystals. In contrast to type-I systems, the ground-state absorption is found to be blueshifted when exciton-hole and exciton-exciton complexes are formed. For a positively charged dot, we argue that this is the consequence of the dominance of the hole-hole interaction compared to the electron-hole interaction due to the spatial separation of the electron and hole. The large oscillator strength (0.5) and the exciton binding energy (25 meV) are determined from the experimental data. The results are explained by effects of the electron and hole localization and by electron wave-function leakage in the dots. The electronic structure of spatially indirect excitons is calculated self-consistently in the effective-mass approximation for pyramidal-shaped Ge/Si quantum dots. The inhomogeneous strain distribution in the quantum dot layer has been taken into account through modification of the confining potential. The calculations show that the electron of an indirect exciton resides in the Si near to the Ge pyramid apex due to maximum strain in this region, while the hole is confined close to the pyramid base. The electron-hole overlap is calculated to be 15%. When two excitons are excited in the dot, the electrons are found to be spatially separated and have different single-particle quantization energies. We argue that this is the reason why the biexciton absorption is blueshifted as compared to a single exciton. A satisfying agreement is found between theoretical and experimental data.

DOI: 10.1103/PhysRevB.63.045312

PACS number(s): 73.21.-b, 73.61.Cw

Ge/Si(001) quantum dots (QD's) exhibit a type-II band lineup. The large (~ 0.7 eV) valence-band offset characteristic of this heterojunction leads to an effective confinement of holes in Ge regions. The holes create a Hartree potential resulting in a triangular quantum well for nonequilibrium electrons in the surrounding Si (Fig. 1). Thus, a fundamental feature of staggered QD's is the spatial separation of electrons and holes resulting in the formation of spatially indirect excitons, whose intriguing properties are still poorly understood. In particular, little is known about the influence of Coulomb interactions on the excitonic properties of charged quantum dots.

In this paper, we use electron-filling modulation absorption spectroscopy (EFA) to study the effect of dot charging on the interband transitions in Ge/Si QD's. Previously, this kind of spectroscopy has been successfully used to study photoluminescence¹ and reflectance² properties of charged InAs and $\text{In}_x\text{Ga}_{1-x}\text{As}$ QD's. In the present experiments, Ge dots are embedded into a n^+p-p^+ Si diode, in which the number of holes in the QD's can be finely tuned by an external applied bias. When a state is occupied by a hole, no interband transition from this state is possible (Fig. 1). When the hole is evacuated from the level, the interband transition is allowed. Modulating the holes in and out of the state by applying an ac bias voltage therefore induces corresponding changes in the infrared absorption. Thus, the absorption signal measured under different bias conditions directly reflects properties of excitons at charged quantum dots.

The sample was grown by molecular beam epitaxy on a (001) oriented $4.5 \Omega \text{ cm}$ boron-doped Si substrate. The growth temperatures for the silicon layers were 800°C and

500°C before and after deposition of the Ge layer, respectively. The growth rates were 2 ML/s for Si and 0.2 ML/s for Ge. The Ge quantum dot layer with a nominal thickness of 10 ML was symmetrically embedded into a $1\text{-}\mu\text{m}$ thick p -Si region (B, $5 \times 10^{16} \text{ cm}^{-3}$) at 300°C . A buried back contact is formed by 50-nm B-doped p^+ -Si ($2 \times 10^{18} \text{ cm}^{-3}$). The structure was finally capped with a 50 nm n^+ -Si front contact (Sb, $1 \times 10^{19} \text{ cm}^{-3}$). The formation of the Ge

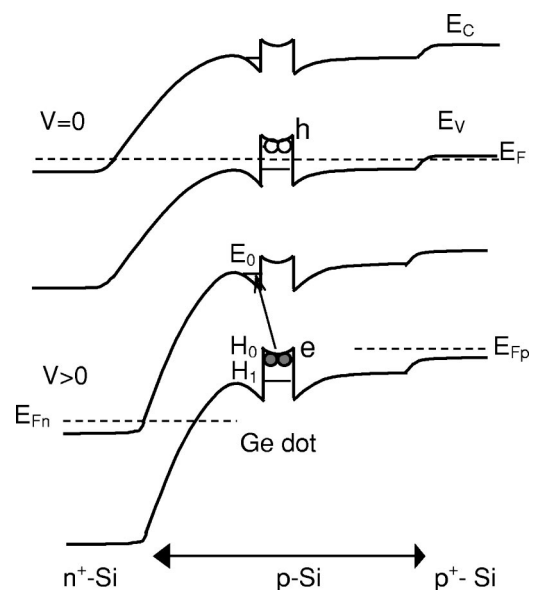


FIG. 1. Schematic of the band diagram of the investigated sample under unbiased and reverse biased conditions.

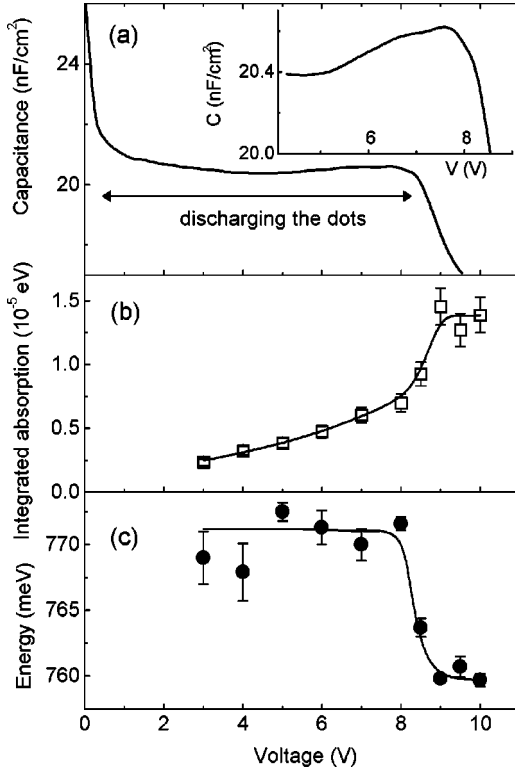


FIG. 2. (a) Capacitance-voltage characteristic measured at $T = 300$ K with a modulation amplitude 10 mV and a modulation frequency 100 kHz. (b) Integrated absorption strength of the H0-E0 transition as a function of bias voltage V_H . (c) Energetic position of the ground-state QD transition in the dark vs applied bias V_H .

QD's was indicated by observing the change in the reflection electron diffraction pattern from streaky to spotty. The structures of similar samples were examined, before deposition of the Si cap layer by scanning tunneling microscopy, and after overgrowth of the cap layer by cross-sectional transmission electron microscopy.³ The dots are pyramidal with base orientation along [100] and [010] directions. The area density of the dots was estimated to be $3 \times 10^{11} \text{ cm}^{-2}$. The average size of the dot base length was found to be about 15 nm, the height about 1.5 nm, and the dot uniformity approximately $\pm 20\%$.

Infrared absorption measurements were performed in normal-incidence geometry on mesa diodes at room temperature. Unmodulated light from a global source illuminated the front side of the diode. The transmitted light then passed through the monochromator and was detected by a Ge photodiode. Differential absorption was measured by applying a reverse bias modulated between a low level V_L and a high level V_H .

The 100 kHz capacitance-voltage (CV) characteristic measured at 300 K is shown in Fig. 2(a) and illustrates the charge state of the sample investigated. The region of negative slope in the CV curve (at $V_H = 6-8$ V) is a consequence of the zero dimensionality of states associated with the dots.⁴ To determine the position of the QD layer, we used the approximate relation $x = \epsilon_0 \epsilon_r / C$, where ϵ_r is the relative permittivity. For $C \approx 20 \text{ nF/cm}^2$, the result is $x = 0.5 \text{ } \mu\text{m}$,

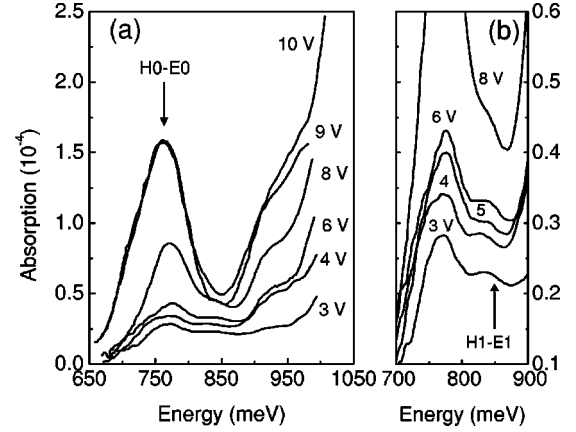


FIG. 3. (a) Room-temperature electron-filling absorption spectra at different reverse bias. (b) Expanded view of the spectra at low bias.

which is in agreement with the nominal position of the Ge layer. The dots are charged with holes at zero bias. The holes begin to escape at $V_H > 0.5$ V and the dots become totally depleted at $V_H > 8.5$ V [Fig. 2(a)]. In the discussion that follows, we modulate the bias voltage between $V_L = 0$ V and $V_H = 2-10$ V. All measured EFA signals were normalized to the source spectrum so that any spectral response not associated with the modulated part of the sample is eliminated from the results. This approach is appropriate for the case of weakly absorbing samples.

Figure 3 shows the EFA signal measured at different values of the bias V_H . Below the energy gap of Si, at energies $\approx 760-770$ meV, we observe an absorption maximum with a Gaussian line shape and a broadening of $\approx 50-70$ meV, which is interpreted as an indirect excitonic transition between the hole ground state (H0) in the Ge dots and the electron ground state (E0) confined in Si near the heterojunction. A similar peak at $\approx 730-750$ meV has been observed previously in the photocurrent spectra of a Ge/Si heterostructure with quantum dots of similar sizes.³ We assume that the broadening of the interband transition is mainly due to the dispersion of the carrier confinement energies of dots with different sizes.

An additional fine structure at ≈ 850 meV is assigned to the transition between the hole excited state (H1) and the electron excited state (E1). The separation of the two hole states in the Ge dot is $\approx 70-80$ meV.^{5,6} The energy difference between the H0-E0 and H1-E1 transitions is ≈ 90 meV. This implies that the separation of the two electron states, $\approx 10-20$ meV, is much smaller than that for the holes. A probable reason is that the holes are confined in a small dot, while the electrons are more spread out.

At higher energies, the absorption gradually increases due to excitations to extended states in the conduction band of Si and Ge, superimposed on the several absorption bumps, which are tentatively attributed to transitions between highly excited states in the dots or in the wetting layer. To make a careful analysis of the absorption edges, one should take into account the energy dependence of the absorption coefficient for spatially indirect transition from a confined state to a

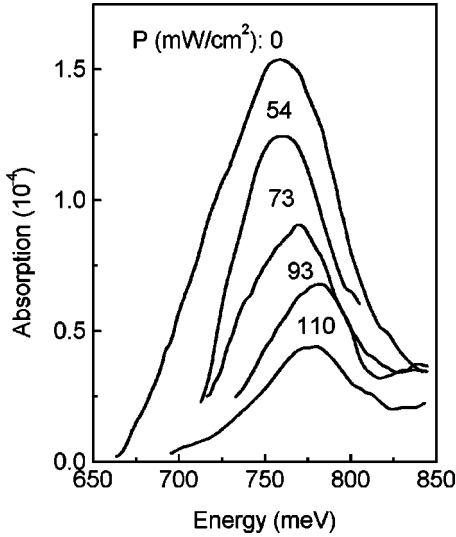


FIG. 4. Effect of optical pumping on the EFA spectra at different pump intensities. The modulation bias amplitude is fixed at $V_H = 9$ V.

delocalized band. Since a theoretical treatment of such a dependence is a formidable task, we will not make this analysis in the present paper.

It is of importance to relate the absorption spectra to other data on Ge/Si nanostructures. Photoluminescence (PL) measurements have been performed to determine the energy of excitonic transitions in Ge/Si self-assembled islands.^{7,8} Ge dot related luminescence is usually observed at ≈ 800 meV, which is consistent with the position of the absorption line observed in this work.

The assignment of the peak near 750 meV to the H0-E0 transition is supported by analysis of the integrated absorption I as a function of V_H [Fig. 2(b)]. (I is obtained by calculating the areas under Gaussians fitted to the absorption peaks.) In our geometry

$$I = h e^2 n f / 2 m_0 \epsilon_0 c (1 + \sqrt{\epsilon_r}), \quad (1)$$

where n is the density of electrons in the highest valence-band state of the Ge dots, f is the oscillator strength, and c is the speed of light. Since $I \propto n$, the $I - V_H$ curve illustrates the change in the charge state of the dots. At $V_H > 8.5$ V, the integrated absorption does not depend on the voltage. Below 8.5 V, the EFA intensity weakens indicating a decrease in the number of modulated electrons in the valence band of the dots, in agreement with the CV measurements.

To obtain further evidence to support the proposed origin of the EFA peak, we have studied the effect of additional interband optical excitation of the sample by a tungsten halogen lamp with a bandpass filter as the source. The absorption spectra obtained at a fixed modulation voltage ($V_H = 9$ V) and at different pump excitation densities are depicted in Fig. 4. When the sample is illuminated, nonequilibrium electrons and holes are photogenerated. The holes are captured by the dots, while the electrons are accumulated near the dots forming the indirect excitons. At high pump intensities, the hole and electron ground states become fully occupied and the

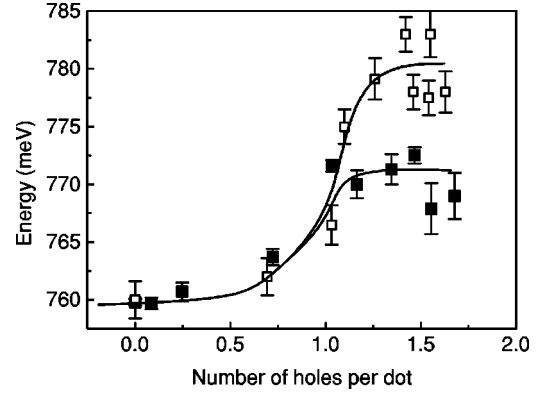


FIG. 5. Ground-state transition energy as a function of the hole occupation per dot. The data were taken at different bias in the dark (solid squares), and at different pump intensities at fixed bias voltage ($V_H = 9$ V, open symbols).

Pauli exclusion principle forbids the H0-E0 transition. One can see in Fig. 4 that the experimental EFA signal is strongly suppressed by the optical pumping.

The integrated absorption at $V_H > 8.5$ V can be used to determine the oscillator strength per dot. For the H0-E0 transition, the density of absorbers is twice the dot density. (The maximum occupation of the ground state is two.) From the measured value $I \approx 1.4 \times 10^{-5}$ eV, we find $f = 0.5$. This value is more than 20 times less than that obtained for direct excitons in InAs/GaAs QD's (10.9).⁹ Such a difference is not unreasonable since the difference between the two types of QD's is large. Similar conclusions were reached in Ref. 10 from analysis of the PL time decay of type-II GaSb/GaAs QD's. Large values of the oscillator strength and the exciton binding energy for type-II quantum dots with finite offsets was predicted by Rorison.¹¹ They are explained by two aspects of the system. The first is the localization of one of the particles, which allows the other particle of the exciton to correlate more strongly with it. The second is leakage of the wave functions into the barrier regions allowing greater overlap of electron and hole wave functions.

One of the results is that the H0-E0 transition shows a substantial stepwise blueshift of about 11 meV with decreasing reverse bias [Fig. 2(c)]. A qualitatively similar effect is seen with increasing the pump excitation density at fixed V_H (Fig. 4). This result differs drastically from what has been observed for direct excitons, in which case charging leads to a redshift of the excitonic transition.^{9,1} It can be seen in Fig. 2(c) that the transition energy begins to increase when holes are injected into the originally empty QD's. From the oscillator strength obtained above and the measured integrated absorption, we calculate the number of holes per dot N_h at different biases in the dark and at different pump intensities. The energetic position of the indirect excitonic transition is shown in Fig. 5 as a function of N_h . It should be noted that the transition energy increases sharply when the first hole enters the ground state and then is approximately insensitive to further increase in the hole concentration.

The QD's are located in the space-charge region of a pn diode and, therefore, are subjected to a relatively strong electric field. As is well known from the quantum confined Stark

effect (QCSE), an electric field can affect the energetic position of QD's states. We find three arguments against interpretation of the experimental data in terms of the QCSE. First, the Stark shift should be continuous with the field strength. However, we observe that the position of the absorption changes sharply at 8.5 V and then is constant at higher bias. Second, a field induced energy shift should be weak since the height of the QD's in the field direction is only 1.5 nm. Recently Miesner *et al.*⁸ have observed a QCSE of about 60–70 meV at 5 V for 7.5-nm-height Ge/Si QD's. Since the dependence of the QCSE on the width w of the quantum well is established to be very strong [$\sim w^4$ (Ref. 12)], we expect only a negligible Stark shift of ≈ 0.1 meV in the investigated sample. Third, when the external electric field is increased in Ge/Si QD's, a blueshift of the excitonic transition is expected from the experiments of Miesner *et al.*⁸ However, we observe a redshift with increasing bias voltage [Fig. 2(c)]. Thus, we conclude that charging, and not the quantum confined Stark effect, is responsible for the observed energy shift.

When a H0-E0 exciton is created in a positively charged dot, an exciton-hole complex is formed consisting of two holes in the dot and an electron confined near the dot. There are two additional contributions to the energy of the exciton-hole complex as compared to e - h excitation in a neutral dot.⁹ The first is a positive Coulomb energy due to correlation between the two holes in the dot, E_{hh} , and the second is a negative contribution from the Coulomb attraction between the excited electron in the nearby silicon and the second hole on the dot, E_{eh} . Here, we neglect the exchange interaction between the two holes since they have antiparallel spin orientation.¹³ For direct excitons, the electron-hole interaction dominates and the resulting shift $\Delta E_{h-ex} = E_{hh} - E_{eh}$ is negative.⁹ Hence the expected reduction of the overlap factor for type-II excitons as compared with type-I systems yields a smaller magnitude of the electron-hole interaction energy E_{eh} . As a result, the energy of the exciton-hole interaction referenced to a neutral exciton energy can be positive. Taking the experimentally observed shift of 11 meV and the h - h interaction energy $E_{hh} = 36$ meV (determined by capacitance spectroscopy in Ref. 4), the exciton binding energy is determined to be $E_{eh} = 25$ meV. Note that this value is larger than the free-exciton binding energy in the bulk Si (≈ 10 meV), in agreement with the Rorison's arguments.¹¹ On the other hand, E_{eh} is much smaller than E_{hh} , which agrees with the fact that the electron is separated from the hole (and less localized than the hole).

As can be seen from Fig. 5, optical pumping affects the transition energy more strongly than the bias voltage. This stems from the fact that illumination creates both holes and electrons while the field effect only induces holes in the dots. Under illumination, we have two interacting excitons in the dot: the first is generated by the pump illumination; the second is excited by the infrared probing light. As compared to a single exciton, the transition energy now increases by

$$\Delta E_{ex-ex} = E_{ee} + E_{hh} - 2E_{eh}, \quad (2)$$

where E_{ee} is the energy of repulsive interaction between two electrons confined near the dot. For ΔE_{ex-ex}

$= 20$ meV, $E_{hh} = 36$ meV, and $E_{eh} = 25$ meV, we obtain a surprising result $E_{ee} = 34$ meV. It is quite improbable that E_{ee} could be so close to E_{hh} in a system where the hole states are more localized than the electron states. To resolve this problem we make self-consistent calculations of the expected electronic structure.

To obtain theoretical estimates of the oscillator strength and all Coulomb energies of the system under investigation, a realistic Ge nanocrystal geometry has to be used for model calculations. We consider a $\{105\}$ -faceted Ge pyramid with a square base in the (001) plane and with base length of 15 nm and height of 1.5 nm. The nanocrystal rests on a 5 ML thick Ge wetting layer and is entirely surrounded by Si. In the discussion that follows, the z axis is taken to be along the principle axis of symmetry of the pyramid. The x and y axes lie in the plane of the wetting layer.

First of all, the strain distribution inside and around QD was calculated using the valence force field (VFF) model with the Keating potential.¹⁴ The VFF model is a microscopic theory that includes bond stretching and bond bending, and avoids the potential failure of the elastic continuum theory in the microscopic limit. Then the strain-induced modifications of the conduction and valence bands of Ge and Si were obtained by using deformation potentials given in Ref. 15. As a result of the strain, the sixfold degeneracy of the conduction-band minima in Si is lifted to give two lowest Δ minima, oriented along $[001]$ and $[00\bar{1}]$ directions and lying lower than those in Ge.

In order to investigate the excitonic properties, a set of three-dimensional, self-consistent effective-mass Schrödinger equations was solved for electrons and holes using the Hartree approximation. The set contains two equations for a single exciton, three equations for an exciton-hole complex, and four equations for two excitons at the dot. The interaction between charged particles was modeled by a statically screened Coulomb potential: $U_{ij}(\mathbf{r}_i, \mathbf{r}_j) = e^2/4\pi\epsilon_0|\mathbf{r}_i - \mathbf{r}_j|$. In the conduction band, the band offset between Δ minima of unstrained Ge and Si is taken equal to 340 meV. In the valence band, the band offset without strain is 610 meV. The effective mass both in the conduction and the valence bands is decoupled between the growth axis and the layer plane. The effective mass in the conduction band of Si is $m_z = 0.92m_0$ and $m_{xy} = 0.19m_0$. In the valence band of Ge, the effective mass is taken equal to $m_z = 0.2m_0$ and $m_{xy} = 0.39m_0$. Only the heavy-hole states are considered in the valence band, since the light-hole states lie close to the valence-band edge.

The confining potentials for electron and hole along the z axis in the structure and the carrier wave functions are given in Fig. 6(a). Figure 6(b) shows the isosurfaces of the electron and hole wave functions. Note that the electron is localized near the pyramid apex, where the strain is maximum. The electron-hole overlap is calculated to be 15%. If we take an electron-hole overlap of 80% for type-I InAs/GaAs QD (Ref. 16) and an oscillator strength of 10.9 as observed also for InAs/GaAs,⁹ we expect for the dots with an electron-hole overlap of 15% to have an oscillator strength of about 0.38,

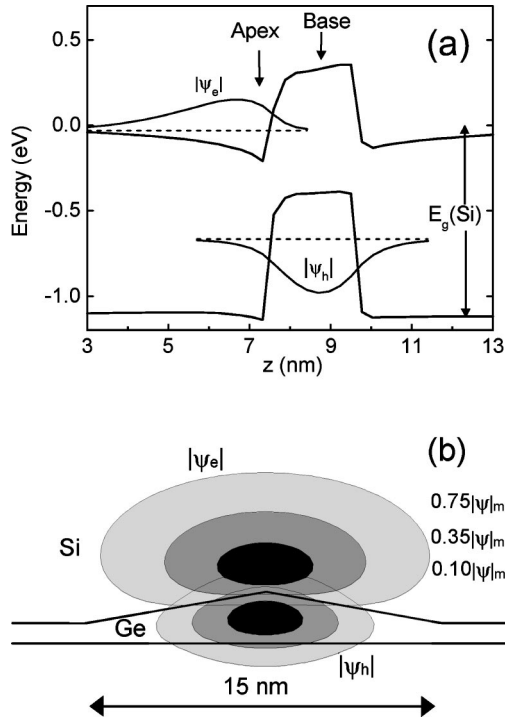


FIG. 6. The confining potentials and the wave functions for electron and heavy hole along the principle axis of symmetry in the dot (a). Isosurface plots of the electron and hole states (b).

in a reasonable agreement with experiment (0.5). This strong oscillator strength of the Ge QD's can be explained by electron leakage in the dots.

The experimental and calculated values of all interaction energies are listed in Table I. The electron-hole interaction energy is calculated to be 31 meV, in a reasonable agreement with the exciton binding energy found experimentally (25 meV). As compared to a single exciton, the expected blue-shift of the excitonic transition for the exciton-hole complex is determined to be 8 meV, which agrees with the experimental value 11 meV (Fig. 5).

The calculations were extended to examine the structure of the exciton-exciton complex. In Fig. 7 we depict the calculated potential profiles and the wave functions for two excitons in the dot. It would be worth mentioning that the two electrons in the exciton-exciton complex are *spatially separated*. Electron-electron repulsion causes the second electron to localize below the dot base. As a result, the $e-e$ interaction energy turns out to be only 19 meV, i.e., about two times less than the energy of the $h-h$ interaction. Taking theoretical

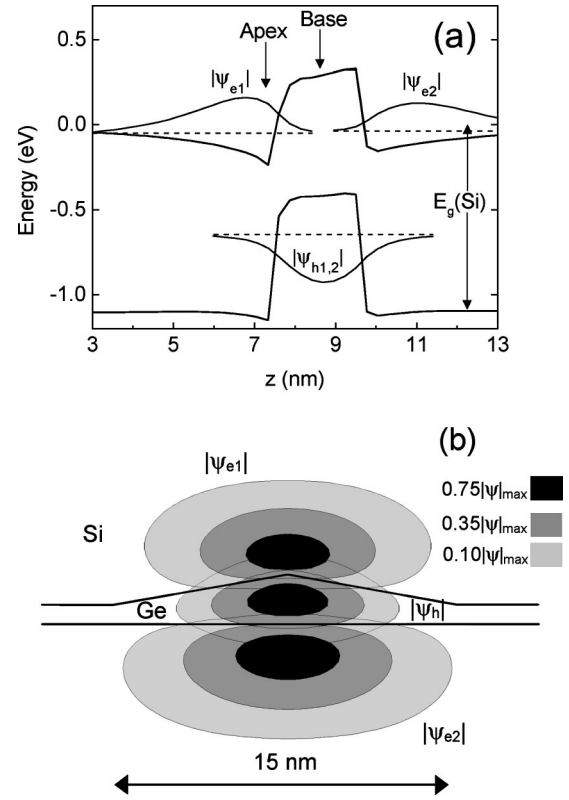


FIG. 7. The confining potentials and the wave functions for two electrons and two holes along the principle axis of symmetry in the dot (a). Isosurface plots of the electron and hole states for a exciton-exciton complex (b).

interaction energies from Table I and using Eq. (2), we find $E_{\text{ex-ex}} = -4$ meV, i.e., the transition for the exciton-exciton complex should be redshifted as compared to a single exciton, in contrast to our observation. In fact, one has to remember that Eq. (2) ignores the difference in kinetic and potential energies of electrons and is valid only when both electrons are localized in the same quantum state. The calculations show that the second (right) potential well for electrons in the conduction band of Si is more shallow than the first one [the left well in Fig. 7(a)] due to a different strain that modifies the band structure. As a result, the single-particle energy of the second electron is larger than that for the first one, and the resulting shift of the absorption $E_{\text{ex-ex}}$ turns out to be positive and equals to 10.2 meV.

In summary, we have used electron-filling modulation absorption spectroscopy to study the interband transitions in

TABLE I. Energy parameters of indirect exciton and excitonic complexes in Ge/Si quantum dots. E_{eh} the exciton binding energy, E_{hh} the interaction energy between two holes in the ground state of the dot, E_{ee} the interaction energy between two electrons in a Hartree potential of two holes, $\Delta E_{\text{ex-h}}$ and $\Delta E_{\text{ex-ex}}$ are the shifts of the excitonic transition for the exciton-hole and exciton-exciton complexes as compared to a single exciton.

Source	E_{eh} (meV)	E_{hh} (meV)	E_{ee} (meV)	$\Delta E_{\text{ex-h}}$ (meV)	$\Delta E_{\text{ex-ex}}$ (meV)
Experiment	25	36	34	+11	+20
Calculation	31	39	19	+8	+10.2

charged type-II Ge/Si quantum dots. When the dots are loaded with holes by changing the reverse bias, the ground-state transition in the absorption spectra shows a stepwise blueshift of about 11 meV accompanied by a decrease in intensity. Interband optical pumping at a fixed bias voltage leads to a shift of about 20 meV. The observed changes are explained by exciton-hole and exciton-exciton interactions. For the case of two excitons in a dot, the blueshift can be explained by the spatial separation of electrons and their localization in different potential wells. Based on the absorption measurements, we have determined the exciton oscillator strength $f=0.5$ and the exciton binding energy 25 meV.

The experimental results are supported by our detailed self-consistent calculations.

The authors would like to acknowledge very useful discussions with John Adkins from Cambridge University. This work was supported by Russian Foundation of Basic Research (Grant No. 00-02-17885), the Interdisciplinary Scientific and Technical Program ‘‘Physics of Solid State Nanostructures’’ (Grant No. 98-1100), and the Intercollegiate Scientific Program ‘‘Universities of Russia-Basic Research’’ (Grant No. 015.01.01.34). Research was sponsored in part by the RFBR-SFNS of China under Grant No. 99-02-39051GFEN-a.

-
- ¹K. H. Schmidt, G. Medeiros-Ribeiro, and P. M. Petroff, *Phys. Rev. B* **58**, 3597 (1998).
- ²T. M. Hse, W.-H. Chang, K. F. Tsai, J.-I. Chyi, N. T. Yeh, and T. E. Nee, *Phys. Rev. B* **60**, R2189 (1999).
- ³A. I. Yakimov, A. V. Dvurechenskii, Yu. Yu. Proskuryakov, A. I. Nikiforov, O. P. Pchelyakov, S. A. Teys, and A. K. Gutakovskii, *Appl. Phys. Lett.* **75**, 1413 (1999).
- ⁴A. I. Yakimov, A. V. Dvurechenskii, A. I. Nikiforov, and O. P. Pchelyakov, *Zh. Éksp. Teor. Fiz. Pis'ma Red.* **68**, 125 (1998) [*JETP Lett.* **68**, 135 (1998)]; *Thin Solid Films* **336**, 332 (2000).
- ⁵A. I. Yakimov, C. J. Adkins, R. Boucher, A. V. Dvurechenskii, A. I. Nikiforov, O. P. Pchelyakov, and G. Biskupski, *Phys. Rev. B* **59**, 12 598 (1999).
- ⁶A. I. Yakimov, A. V. Dvurechenskii, N. P. Stepina, and A. I. Nikiforov, *Phys. Rev. B* **62**, 9939 (2000).
- ⁷H. Sunamura, N. Usami, Y. Shiraki, and S. Fukatsu, *Appl. Phys. Lett.* **66**, 3024 (1995); E. Palange, G. Capellini, L. Di Gaspare, and F. Evangelisti, *ibid.* **68**, 2982 (1996); Feng Liu and M. G. Lagally, *Surf. Sci.* **386**, 169 (1997); S. Fukatsu, H. Sunamura, Y. Shiraki, and S. Komiyama, *Appl. Phys. Lett.* **71**, 258 (1997); P. A. M. Rodrigues, F. Cerdeira, and J. C. Bean, *ibid.* **75**, 145 (1999).
- ⁸C. Miesner, O. Röthig, K. Brunner, and G. Abstreiter, *Physica E (Amsterdam)* **7**, 146 (2000).
- ⁹R. J. Warburton, C. S. Dürr, K. Karrai, J. P. Kotthaus, G. Medeiros-Ribeiro, and P. M. Petroff, *Phys. Rev. Lett.* **79**, 5282 (1997).
- ¹⁰F. Hatami, M. Grundmann, N. N. Ledentsov, F. Heinrichsdorff, R. Heitz, J. Böhrer, D. Bimberg, S. S. Ruvimov, P. Werner, V. M. Ustinov, P. S. Kop'ev, and Zh. I. Alferov, *Phys. Rev. B* **57**, 4635 (1998).
- ¹¹J. M. Rorison, *Phys. Rev. B* **48**, 4643 (1993).
- ¹²G. Bastard, E. E. Mendez, L. L. Chang, and L. Esaki, *Phys. Rev. B* **28**, 3241 (1983).
- ¹³A. Wojs and P. Hawruluk, *Phys. Rev. B* **55**, 13 066 (1997).
- ¹⁴A. V. Nenashev and A. V. Dvurechenskii, *JETP* **91**, 497 (2000).
- ¹⁵C. G. Van de Walle, *Phys. Rev. B* **39**, 1871 (1989).
- ¹⁶M. Grundmann, O. Stier, and D. Bimberg, *Phys. Rev. B* **52**, 11 969 (1995).